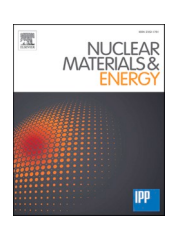
ELSEVIER

Contents lists available at ScienceDirect

## **Nuclear Materials and Energy**

journal homepage: www.elsevier.com/locate/nme



# Refined guiding centre approximation for kinetic studies of Nitrogen seeding in medium density ITER L-mode scenarios with EMC3-EIRENE

D. Harting <sup>a,\*</sup>, A. Knieps <sup>a</sup>, D. Reiser <sup>a</sup>, S. Rode <sup>a</sup>, J. Romazanov <sup>a</sup>, P. Börner <sup>a</sup>, Y. Feng <sup>b</sup>, H. Frerichs <sup>c</sup>

### 1. Introduction

Impurity seeding in the scrape off layer plasma as well as controlling the contamination of the core plasma by high Z impurities are essential for ITER baseline scenarios. Predictions for the ITER baseline scenarios are often based on fluid descriptions of the impurity transport. However, especially lower ionization stages of high Z impurities (e.g. Ar, W) do not have the time to equilibrate to a Maxwellian velocity distribution and a kinetic treatment might be more appropriate than a fluid description for these short-lived ionization stages.

To simulate kinetic effects of impurities, the EMC3-EIRENE [1,2] code package was recently extended by a kinetic ion transport module in guiding centre approximation [3]. The kinetic ion transport module is part of the kinetic neutral Monte Carlo code EIRENE [4] and currently contains grad-B and curvature drifts including mirror-force effects, anomalous cross-field diffusion and a simplified model for Coulomb collisions via an ion-ion energy loss frequency in Langer approximation. In this paper we present improvements and verifications of the kinetic ion transport module of EMC3-EIRENE by reproducing basic properties of the guiding centre approximation together with an application for Nitrogen seeding in an ITER medium density L-mode scenario.

## 2. Kinetic ion transport model

The Kinetic ion transport module of EMC3-EIRENE is based on a guiding centre model in trace ion approximation. Currently the EMC3 code includes only an approximated parallel electric field based on a simplified momentum balance for the electrons. For this reason, we are currently not taking into account any  $\vec{E} \times \vec{B}$  drift or acceleration of the kinetic ions in the electric field. As a next step in the future, we plan to include at least the acceleration due to the simplified parallel electric field in the kinetic ion transport module of EMC3-EIRENE. This would be

in line with the existing trace fluid impurity model already present in the EMC3 code. The kinetic ion transport module currently lacks also any contribution from thermal and friction force effects. This is foreseen to be dealt with in future improvements to the Coulomb collision model. With the neglection of the electric field, the guiding centre velocity for the kinetic ions in the EMC3-EIRENE code is then given by equation (1).

$$\vec{V}_{gc} = \nu_{\parallel} \frac{\vec{B}}{B} + \frac{\nu_{\parallel}^2 + \nu_{\perp}^2 / 2}{q_i B / m_i} \frac{\vec{B} \times \vec{\nabla} B}{B^2}$$
 (1)

The change of the parallel and perpendicular velocity components can be derived from the conservation of the magnetic moment and energy and has also a contribution from the Coulomb collisions.

$$\dot{v}_{\parallel} = -\frac{v_{\perp}^{2}}{2} \frac{\nabla_{\parallel} B}{R} + Coulomb \ collisions \tag{2}$$

$$\dot{v}_{\perp} = \frac{v_{\parallel}v_{\perp}}{2} \frac{\nabla_{\parallel}B}{B} + Coulomb \ collisions \tag{3}$$

The guiding centre transport is then described by a stochastic jump process  $\Delta \vec{R}_{\rm gc} = \vec{V}_{\rm gc} \Delta t + \sqrt{D_\perp \Delta t} \vec{\zeta}_\perp$ , where  $\vec{\zeta}_\perp$  is a random unit vector perpendicular to the magnetic field.

The cell geometries of the EMC3 and EIRENE codes are shown in Fig. 1, where a field line in the EMC3 cell can be represented by local coordinates  $u^1$ ,  $u^2$ . Both cell representations share the same corner points, but as the EIRENE code internally works with Cartesian coordinates, the corner points of the EIRENE cell are connected by straight lines and the cell surface is represented by triangles.

For a starting point  $\overline{P}_1$  of a trajectory in the current cell, the point  $\overline{P}_2$  where the particle would leave the cell only due to parallel transport is calculated together with the traveling time  $\Delta t_{\parallel}$  in the curved field line representation of the EMC3 cell. These two points are transformed back to Cartesian coordinates and define a local parallel Cartesian

E-mail address: d.harting@fz-juelich.de (D. Harting).

a Forschungszentrum Jülich GmbH, Institut für Energie- und Klimaforschung – Plasmaphysik, Partner of the Trilateral Euregio Cluster (TEC), 52425 Jülich, Germany

<sup>&</sup>lt;sup>b</sup> Max Planck Institute for Plasma Physics, 17491 Greifswald, Germany

<sup>&</sup>lt;sup>c</sup> University of Wisconsin - Madison, Department of Engineering Physics, WI, USA

<sup>\*</sup> Corresponding author.

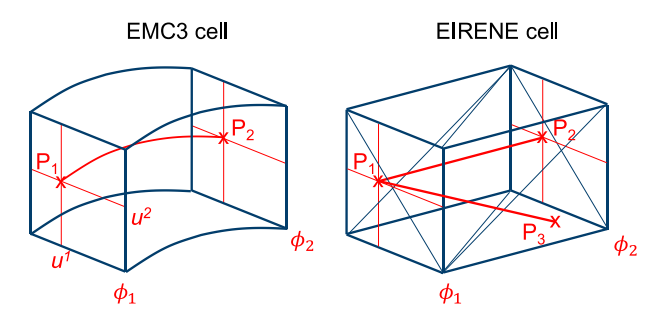
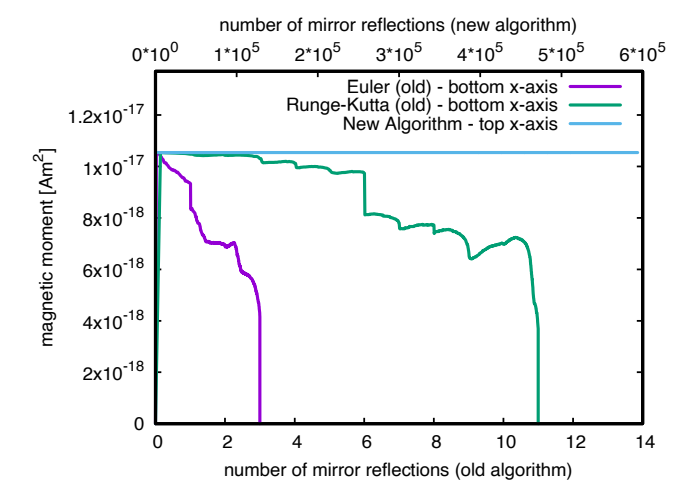


Fig. 1. Cell representation in the EMC3 (left) and the EIRENE (right) code.



**Fig. 2.** Conservation of the magnetic moment for the old Euler and Runge-Kutta method (on bottom x-axis) and the new integration method (on top x-axis).

velocity vector  $\vec{V}_{\parallel} = \left(\vec{P}_2 - \vec{P}_1\right) \bigg/ \Delta t_{\parallel}$ . Additionally an 'effective diffusion velocity' in Cartesian coordinates is defined by  $\vec{V}_{diff} = \left(\sqrt{D_{\perp}\Delta t_{\parallel}}\,\vec{\zeta}_{\perp}\right) \bigg/ \Delta t_{\parallel}$  and together with the drift velocity  $\vec{V}_{drift} = \frac{v_{\parallel}^2 + v_{\perp}^2/2}{q_1B/m_1} \frac{\vec{B} \times \vec{\nabla} B}{B^2}$  the step velocity is defined by  $\vec{V}_{step} = \vec{V}_{\parallel} + \vec{V}_{drift} + \vec{V}_{diff}$ . The particle is then advanced in Cartesian coordinates with the final timestep  $\Delta t_{cut}$  to the intersection point  $\vec{P}_3$  with the cell surface (or to a mean free path event inside of the cell) by  $\vec{P}_3 = \vec{P}_1 + \vec{V}_{step}\Delta t_{cut}$ . This is only approximately correct for  $\Delta t_{cut} \approx \Delta t_{\parallel}$ , as the diffusion jump step is not scaling linearly with  $\Delta t$ . A better treatment where the diffusive step is separated from the convective step is discussed later in section 4.

## 3. Conservation of the magnetic moment

After the final Point  $\overline{P}_3$  of the transport step and the traveling time  $\Delta t_{cut}$  was calculated, the change of the parallel velocity is estimated by solving the ODE (2) without the contribution from the Coulomb collisions. The change in the perpendicular velocity is given by the energy conservation. The original implementation of the kinetic ion transport module in EIRENE provides two integration methods to solve the ODE, a simple Euler and a Runge-Kutta method. To verify the kinetic ion transport module, we have launched a particle in the magnetic mirror on the outer midplane and switched off all contribution from drifts, diffusion and Coulomb collisions. The evolution of the magnetic moment for both existing integration methods are shown in Fig. 2, where the magnetic moment is plotted versus the number of mirror reflections (bottom x-axis) the particle has experienced. Both existing integration methods

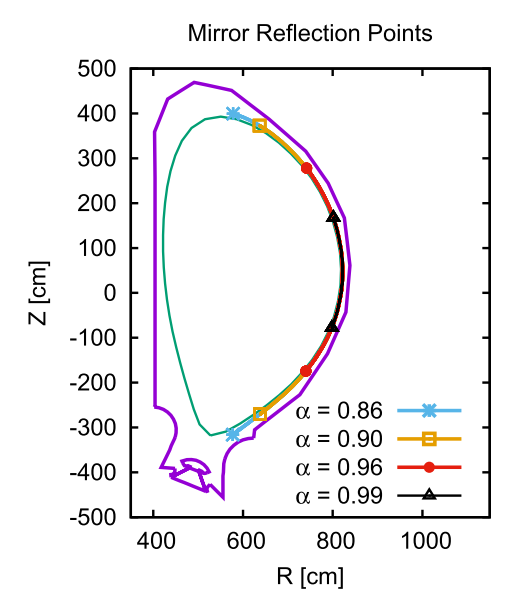


**Fig. 3.** Trajectories and reflection points in the magnetic mirror for particles launched at the OMP with different trapping condition  $\alpha$ . Drifts, diffusion and Coulomb collisions were switched off.

are not conserving the magnetic moment. The particle is lost out of the magnetic mirror after two mirror reflections by the existing Euler integration method (purple curve) and after ten mirror reflection by the existing Runge-Kutta integration method (green curve).

We have designed now a new method which enforces the conser-

vation of the magnetic moment and energy directly (blue curve in Fig. 2). As the final Point  $\overrightarrow{P}_3$  of the step is already known, we do not need to solve the ODE (2), but instead directly calculate the final parallel and perpendicular velocity components by utilizing the conservation of magnetic moment and energy. With the velocities  $v_{\parallel 1}$ ,  $v_{\perp 1}$  and the magnetic field strength  $B_1$  at the starting Point  $\overrightarrow{P}_1$  together with the magnetic field strength  $B_3$  at the final Point  $\overrightarrow{P}_3$  we get from the conservation of the magnetic moment  $v_{\perp 3}^2 = v_{\perp 1}^2 B_3/B_1$  and with the conservation of energy  $v_{\parallel 3}^2 = v_{\parallel 1}^2 + v_{\perp 1}^2 - v_{\perp 3}^2$ . Here we need to ensure that the squared parallel velocity  $v_{\parallel 3}^2$  at the final point  $\overrightarrow{P}_3$  is not becoming negative and instead a mirror reflection is triggered which switches the sign of the parallel motion. The result for the new algorithm is show in the blue curve of Fig. 2 which is related to the top x-axis (different scaling than bottom x-axis). As expected, the magnetic moment is now fully conserved and no loss of the magnetic moment is observed even for more than  $6 \times 10^5$  mirror reflections.

As another verification of the new algorithm, we again switched off all contributions from drifts, diffusion and Coulomb collisions and launched particles in the magnetic mirror at the outer midplane (OMP) with different trapping conditions  $\alpha = \frac{|\nu_{\perp}|}{|\nu|} > \sqrt{\frac{B_{min}}{B_{max}}}$ . The trajectories of the particles are plotted in Fig. 3 which show a smaller or larger extent in the magnetic mirror depending on their trapping condition  $\alpha$ . The reflection points are stable and do not drift over several hundred thousand mirror reflections. For each particle, we have logged the magnetic field strength along its trajectory and used the maximum and minimum values to reconstruct the trapping condition  $\alpha$ . The reconstructed trapping conditions  $\alpha = 0.8585, 0.8983, 0.9598, 0.9892$  are very close to the ones used to launch the particles (0.86, 0.90, 0.96, 0.99), which means that the mirror reflections happen at the correct magnetic field strength.

### 4. Banana orbits

To further verify the kinetic ion transport module of EMC3-EIRENE

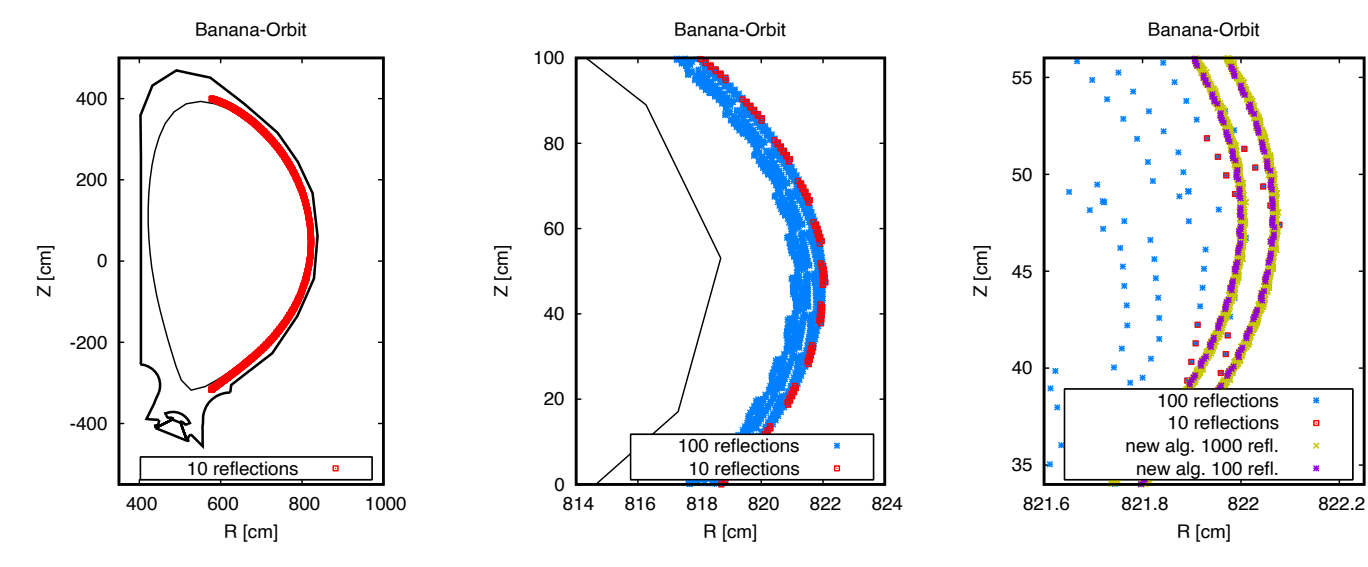


**Fig. 4.** Left plot: Trajectory of the trapped ion in the magnetic mirror for 10 mirror reflections. Centre plot: Zoom at OMP shows large numerical diffusion of a trajectory with the old algorithm for 100 mirror reflections. Right plot: Further zoom at OMP shows stable formation of banana orbits with the new algorithm in local curvilinear coordinates for 100 and 1000 mirror reflections.

we consider the formation of banana orbits in the magnetic mirror due to the grad-B drift. For this we switch off Coulomb collisions and anomalous cross field diffusion and switch on the grad-B and curvature drifts. The kinetic ion is launched at the outer midplane with an energy of 140 eV and a trapping condition  $\alpha=0.86$ . The left plot of Fig. 4 shows the trajectory of the trapped ion for 10 mirror reflections (red symbols). The centre plot of Fig. 4 is a zoom into the outer midplane region together with a longer trajectory covering 100 mirror reflections (blue symbols). We can see that the longer trajectory has a strong numerical diffusion which is attributed to inaccuracies in the Cartesian representation of the drift motion.

We have now completely redesigned the particle motion of the kinetic ions in the EMC3-EIRENE code. The new algorithm for the particle motion is no longer working in Cartesian coordinates but uses now the local curvilinear coordinate system  $\vec{u}=u^1\vec{e}_1+u^2\vec{e}_2+u^3\vec{e}_3$  of the EMC3 cell (Fig. 1) where  $\vec{e}_3$  is parallel to the magnetic field. With the contravariant components  $w^1$ ,  $w^2$  and  $w^3$  of the combined grad-B and curvature drift velocity vector  $\vec{V}_{drift}$  we have a system of ordinary differential equations for the particle motion in the local curvilinear coordinates of the EMC3 cell.

$$\begin{split} \frac{du^{1}}{dt} &= w^{1}\left(u^{1}, u^{2}, u^{3}\right) \\ \frac{du^{2}}{dt} &= w^{2}\left(u^{1}, u^{2}, u^{3}\right) \\ \frac{du^{3}}{dt} &= \frac{\sigma}{\sqrt{g_{33}}} v_{\parallel}\left(u^{1}, u^{2}, u^{3}\right) + w^{3}\left(u^{1}, u^{2}, u^{3}\right) \end{split}$$

Here  $g_{33}=\vec{e}_3\cdot\vec{e}_3$  is the metric coefficient and  $\sigma=-1,+1$  indicating the direction (sign) of the parallel motion. The parallel velocity  $\nu_{\parallel}(u^1,u^2,u^3)$  is given by the energy and magnetic moment conservation as described in section 3. This system of ordinary differential equations is solved by a Runge-Kutta method with adaptive step size control. The result from the new algorithm is shown in the right plot of Fig. 4 for a particle with 100 (purple symbols) and 1000 (yellow symbols) mirror reflections which are now forming stable banana orbits. The small numerical diffusion observed with the new algorithm after 1000 mirror reflections can be roughly estimated by the spreading  $\Delta x=1\times 10^{-4} \mathrm{m}$  of the yellow symbols in the banana orbit over 1000 mirror reflections and the corresponding travelling time  $\Delta t=3.48 \mathrm{s}$ . This gives an estimate of

Table 1 Molecular processes of the AMJUEL database used for Nitrogen molecules  $N_2$  and molecular ions  $N_2^+$  in the simulation.

AMJUEL 2.7.5:	$e + N_2 \rightarrow e + N + N$
AMJUEL 2.7.9:	$e+N_2\rightarrow e+N_2^++e$
AMJUEL 2.7.10:	$e + N_2 \rightarrow e + N + N^+ + e$
AMJUEL 2.7.11:	$e+N_2^+{ ightarrow}e+2N^++e$

the numerical diffusion coefficient of  $D_{\text{numeric}} = \Delta x^2/\Delta t = 2.9 \times 10^{-9}\,\text{m}^2\text{s}^{-1}$  which is orders of magnitude smaller than the typical anomalous perpendicular diffusion of  $D_\perp = 0.3\,\text{m}^2\text{s}^{-1}$  and thus negligible in the final simulations including anomalous perpendicular transport.

While we were redesigning the algorithm for the particle motion, we have also split off the diffusive step from the convective particle motion. As mentioned already in section 2, the original algorithm was linearly rescaling the diffusion step with the final time step  $\Delta t_{cut}$  which is incorrect as the diffusive step scales only with  $\sqrt{\Delta t}$ . The new algorithm is now calculating the time step  $\Delta t_{cut}$  to reach the cell boundary (or a mean free path event inside of the cell) purely on the convective parallel velocity and drift motion. In a second split step this time step  $\Delta t_{cut}$  is used to calculate the random walk step  $\Delta \vec{R}_{\perp} = \sqrt{D_{\perp} \Delta t_{cut}} \vec{\zeta}_{\perp}$  for the perpendicular diffusion, which is treated as a displacement event of the Monte Carlo particle in EIRENE.

## 5. First stable simulations of Nitrogen seeding

With the new developments we are now able to perform the first simulation with the improved kinetic ion transport module of EMC3-EIRENE. We use a plasma background obtained by EMC3-EIRENE for a medium density (attached) ITER L-mode scenario with a separatrix density of  $n_{sep}=1\times10^{19}~{\rm m}^{-3}$  and  $P_{sep}=20$  MW heating power crossing the separatrix from the core. In this plasma background we puff Nitrogen molecules from the top of the machine with a puff strength of  $\Gamma_{puff}=1\times10^{18}\,{\rm s}^{-1}$  and an energy of 0.026 eV. The perpendicular anomalous diffusion coefficient  $D_\perp$  for the kinetic ions was set to 0.3 m²s-¹. We use ADAS 96 [5] ionization and recombination rates for atomic Nitrogen and all ionization stages together with the AMJUEL [6] data for the molecular processes listed in Table 1. The pump is defined as a surface in the pump duct below the dome with an albedo of 0.9928. In the simulations shown

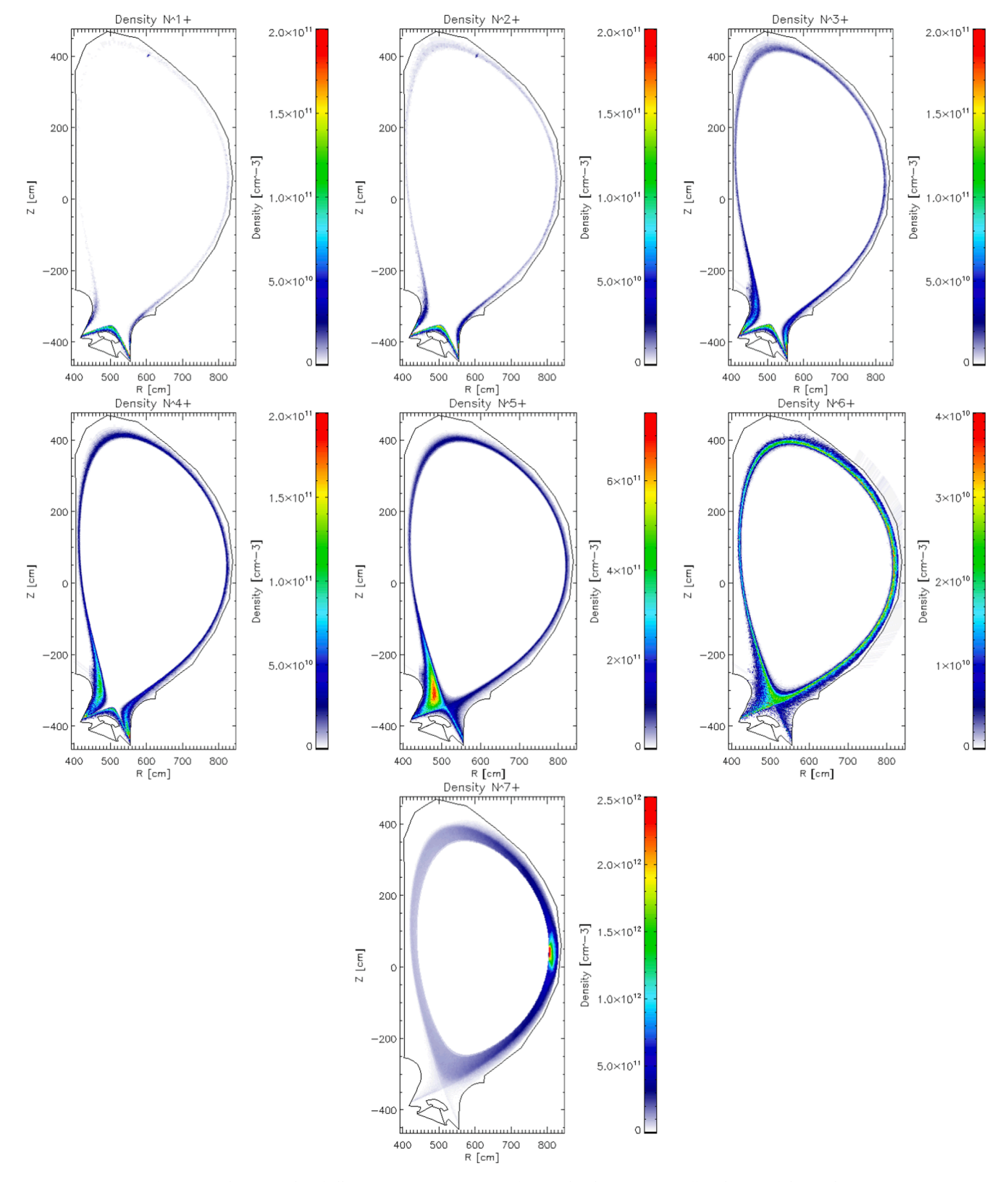


Fig. 5. Simulation results of all Nitrogen ionization stages for a molecular Nitrogen puff at the top of the machine.

here, we launch 150 Monte Carlo particles in the EIRENE code as  $\rm N_2$  molecules from the top of the machines and score their path with a tracklength estimator. This number of Monte Carlo particles seems rather low compared to a typical EIRENE simulation for purely neutral particles, but as Nitrogen is a recycling impurity, the Monte Carlo particles have in this case a very long life-time. Due to the small pump efficiency of the ITER

pump, each Monte Carlo particle will travel the whole simulation volume, enter and escape multiple times the pump region below the dome (where it will lose only a tiny fraction of its weight each time it is hitting the pump surface) and undergo a lot of reflections at the targets and wall (where the kinetic ions recombine to neutral  $N_2$  molecules before they get re-ionized again and continue their flight) until the Monte Carlo particle is

completely absorbed by the pump. The simulation of the 150 Monte Carlo particles took on a single processor (even though the kinetic ion transport module is also MPI parallelized) about 46 h, which corresponds to an average simulation time of about 18 min for each Monte Carlo particle. With this setup, we reached a relative error in the particle balance of 0.01 % and of 0.0001 % in the energy balance. In the simulations shown here, we use the kinetic ion transport module only in a post-processing step. This means that we currently have no feedback e.g. due to radiative cooling to the main plasma. This restriction can be relaxed in the future by using the kinetic ion transport module of EMC3-EIRENE in an iterative way together with the simulation of the plasma background.

The results of the kinetic ion transport simulation with EMC3-EIRENE for all seven ionization stages of Nitrogen are shown in Fig. 5. The lower ionization stages  $N^{I+}-N^{4+}$  are mainly located in the divertor region with higher ionization stages extending further upstream in the scrape of layer. The fifth ionization stage  $N^{5+}$  gets trapped strongly in the magnetic mirror on the high field side of the X-point. The ionization stages  $N^{6+}$  and  $N^{7+}$  need higher electron temperatures and are located more in the closed field line region where  $N^{7+}$  gets trapped in the magnetic mirror at the outer midplane.

The strong trapping of  $N^{5+}$  in the magnetic mirror on the high field side of the X-point and also of  $N^{7+}$  in the magnetic mirror at the outer midplane is exaggerated and probably un-physical. This is due to the fact that EIRENE uses currently a simplified model for Coulomb collisions, which is based on a single energy relaxation time. This simplified Coulomb collision model scales the parallel and perpendicular velocity components of the kinetic ions by the same factor and thus is not changing the trapping condition  $\nu_\perp/\nu > \sqrt{B_{min}/B_{max}}$  of the kinetic ions in the magnetic mirror. This means that the current implementation of the Coulomb collisions in EIRENE do not contribute to the scattering of the kinetic ions into the loss cone of the magnetic mirror as the only loss mechanism from the magnetic mirror is due to perpendicular diffusion. This results in an excessive confinement of the kinetic ions in the magnetic mirror.

For the future, we plan to include a more complete model for the Coulomb collisions based on the work presented in [7], which would allow for a scattering of the kinetic ions due to Coulomb collisions into the loss cone of the magnetic mirror.

## 6. Conclusions

We have presented in this paper first verifications for basic properties regarding magnetic moment conservation and formation of banana orbits due to grad-B drifts of the EMC3-EIRENE kinetic ion transport module in guiding centre approximation. We have revealed some serious shortcomings of the original implementation which was not conserving the magnetic moment of the kinetic particles and introduced large numerical diffusion in the grad-B drift. We could demonstrate that redesigning the original algorithm corrected these shortcomings and resulted in an improved kinetic ion transport module of EMC3-EIRENE which is now fully conserving the magnetic moment of the kinetic ions. Furthermore, the numerical inaccuracies in the grad-B and curvature drift implementation were strongly reduced, which allows now for the kinetic ions to form stable banana orbits.

With the improved kinetic ion transport module of EMC3-EIRENE first stable simulations for Nitrogen puffing in an ITER background plasma could be demonstrated. The simulation showed a strong confinement of the kinetic ions in the magnetic mirror on the high field side of the X-point and on the outer midplane. This was attributed to the simplified Coulomb collision model of EIRENE which is not resolving the scattering of the kinetic ions into the loss cone of the magnetic mirror. As a consequence, the loss channel from the magnetic mirror is currently underestimated in the kinetic ion transport module of EMC3-EIRENE and comes only from the perpendicular anomalous diffusion. For the next step, we plan to implement a better treatment of the Coulomb

collisions as described in [7] into the EIRENE code which would provide a proper scattering of the kinetic ions into the loss cone of the magnetic mirror. A similar treatment was already implemented into the guiding centre approximation module of the full gyro-orbit code ERO2.0 [8]. This will allow for the future a detailed cross-benchmark of the ERO2.0 code with the kinetic ion transport module of EMC3-EIRENE. The EMC3 code has also a simplified fluid model for a single impurity species included. As an additional check for the new kinetic ion transport module of EMC3-EIRENE, we plan also for the future a comparison between the existing fluid impurity model of EMC3 and the new kinetic ion transport module of EMC3-EIRENE.

### CRediT authorship contribution statement

D. Harting: Conceptualization, Methodology, Software, Validation, Formal analysis, Investigation, Writing – original draft, Visualization, Funding acquisition. A. Knieps: Software, Investigation, Resources. D. Reiser: Conceptualization, Methodology, Resources, Validation, Writing – review & editing, Supervision. S. Rode: Methodology, Resources. J. Romazanov: Methodology, Validation, Resources. P. Börner: Software, Resources, Data curation. Y. Feng: Software, Resources, Data curation. H. Frerichs: Software, Resources, Data curation.

### **Declaration of Competing Interest**

The authors declare the following financial interests/personal relationships which may be considered as potential competing interests: [Derek Harting reports was provided by EUROFusion. Derek Harting reports a relationship with EUROFusion that includes: funding grants.].

### Data availability

The authors do not have permission to share data.

## Acknowledgements

The authors gratefully acknowledge the computing time granted through JARA on the supercomputer JURECA [9] at Forschungszentrum Jülich.

This work has been carried out within the framework of the EURO-fusion Consortium, funded by the European Union via the Euratom Research and Training Programme (Grant Agreement No 101052200 - EUROfusion). Views and opinions expressed are however those of the author(s) only and do not necessarily reflect those of the European Union or the European Commission. Neither the European Union nor the European Commission can be held responsible for them.

### References

- [1] Y. Feng, F. Sardei, J. Kisslinger, 3D fluid modelling of the edge plasma by means of a monte carlo technique, J. Nucl. Mater. 266–269 (1999) 812–818, https://doi.org/ 10.1016/S0022-3115(98)00844-7.
- [2] Y. Feng, H. Frerichs, M. Kobayashi, A. Bader, F. Effenberg, D. Harting, H. Hoelbe, J. Huang, G. Kawamura, J.D. Lore, T. Lunt, D. Reiter, O. Schmitz, D. Sharma, Recent improvements in the EMC3-eirene code, Contrib. Plasma Phys. 54 (4–6) (2014) 426–431, https://doi.org/10.1002/ctpp.201410092.
- [3] F. Schluck, Contributions to Plasma Physics 60 (2020) e201900144.
- [4] D. Reiter, M. Baelmans, P. Boerner, The EIRENE and b2-EIRENE codes, Fusion Sci. Technol. 47 (2) (2005) 172–186, https://doi.org/10.13182/FST47-172.
- [5] Summers, H. P. (2004) The ADAS User Manual, version 2.6 http://www.adas.ac.uk.
- [6] AMJUEL database http://www.eirene.de.
- [7] D. Reiser, Berichte des Forschungszentrums Jülich 3508 (1998)
- [8] S. Rode, J. Romazanov, D. Reiser, S. Brezinsek, C. Linsmeier, A. Pukhov, Implementation and validation of guiding centre approximation into ERO2.0, Contrib. Plasma Phys. e202100172 (2022), https://doi.org/10.1002/ ctpp.202100172.
- [9] Jülich Supercomputing Centre. (2018). JURECA: Modular supercomputer at Jülich Supercomputing Centre. Journal of large-scale research facilities, 4, A132. <a href="http://dx.doi.org/10.17815/jlsrf-4-121-1">http://dx.doi.org/10.17815/jlsrf-4-121-1</a>.